

Method for measuring energy generation and efficiency of dielectric elastomer generators

Rainer Kaltseis,¹ Christoph Keplinger,¹ Richard Baumgartner,¹ Martin Kaltenbrunner,¹ Tiefeng Li,^{2,3} Philipp Mächler,¹ Reinhard Schwödau,¹ Zhigang Suo,² and Siegfried Bauer^{1,a)}

¹Soft Matter Physics, Johannes Kepler University, Altenbergerstrasse 69, A-4040 Linz, Austria

²School of Engineering and Applied Sciences, Harvard University, Cambridge, Massachusetts 02138, USA

³Institute of Applied Mechanics, Zhejiang University, 38 Zheda Road, Hangzhou, Zhejiang 310027, China

(Received 26 July 2011; accepted 27 September 2011; published online 19 October 2011)

Dielectric elastomer generators convert mechanical into electrical energy at high energy density, showing promise for large and small scale energy harvesting. We present an experiment to monitor electrical and mechanical energy flows separately and show the cycle of energy conversion in work-conjugate planes. A specific electrical energy generated per cycle of 102 mJ/g, at a specific average power of 17 mW/g, is demonstrated with an acrylic elastomer in a showcase generation cycle. The measured mechanical to electrical energy conversion efficiency is 7.5%. The experiment may be used to assess the aptitude of specifically designed elastomers for energy harvesting. © 2011 American Institute of Physics. [doi:10.1063/1.3653239]

Dielectric elastomer generators (DEGs) use soft, electrically and mechanically deformable capacitors to convert mechanical into electrical energy.^{1,2} They reverse the mode of operation of dielectric elastomer actuators,³ developed for a wide range of applications including artificial muscles, tunable optics, inertial drive vibrators, and Braille displays.⁴ DEGs potentially enable light and silent harvesting of mechanical energy from small to large scales, e.g., from human gait to wind and ocean waves.⁵ Theoretical estimates show a huge specific electrical energy generated per cycle up to 1.7 J/g with off-the-shelf materials.⁶ DEGs have been employed in the heel of shoes for energy harvesting from walking. Durability in sea water environment and impedance matching of ocean waves and elastomer membranes make DEGs a promising candidate for off-shore wave energy harvesting. Devices avoiding bulky, rigid, and heavy external electronics were demonstrated based on self priming circuits.^{7–9} Despite these achievements, there is still no common method to display the conversion cycles and to assess the specific electrical energy generated per cycle. Reported experimental values range over orders of magnitude from 2.15 to 400 mJ/g.^{1,10,11}

This paper presents an experiment to monitor the electrical and mechanical energy flows separately. The experiment determines the specific electrical energy generated per cycle, the specific average power, and the mechanical to electrical energy conversion efficiency. Following suggestions made in our previous theoretical work,^{2,6} we operate the generator between two charge reservoirs of different voltages and describe the cycle of energy conversion in work-conjugate planes.

The experiment is carried out with a commonly used material and transducer design (Fig. 1(a)). A 3 M™ VHB™ 4910F dielectric elastomer membrane—thickness 1mm, radius 22.5 mm, and mass 1.53g—is coated with compliant

electrodes (carbon grease made of ELBESIL™ B50 silicon oil and carbon black powder from ABCR™ with an average particle size of 0.42 μm). The membrane is mounted on a buffer chamber of volume 350 cm³ and is deformable by pressure and voltage. Such a membrane is a commonly used design of dielectric elastomer transducers.¹² It should be emphasized that our experiment can be performed with other designs of dielectric elastomer transducers. The inflation allows for equal-biaxial stretch in the top region, the deformation mode predicted to yield the highest energy of conversion.¹³ Due to inflation, the area of the membrane expands and the thickness decreases, so that the capacitance of the membrane increases.

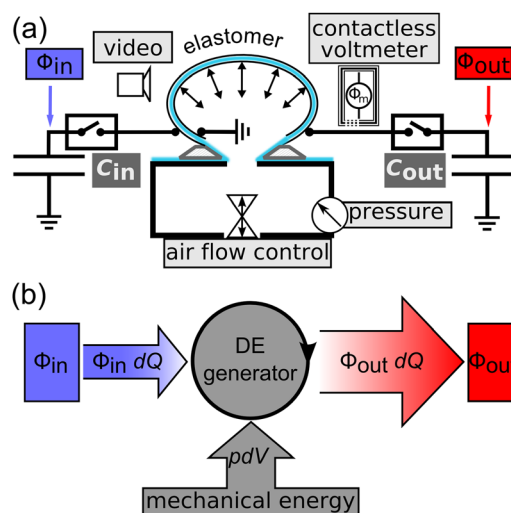


FIG. 1. (Color online) (a) Setup for monitoring electrical and mechanical energy flows in a dielectric elastomer generator. C_{in} and C_{out} serve as input and output charge reservoirs. Electrical and mechanical energy flows are recorded by contactless voltage measurements, pressure sensor readings, and video images of the elastomer shape. (b) Sketch of the electrical and mechanical energy flows in a DEG. Mechanical energy pdV is used to boost the electrical energy from $\Phi_{in}dQ$ to $\Phi_{out}dQ$.

^{a)}Electronic mail: sbauer@jku.at.

We monitor the mechanical energy flows by tracking the excess pressure p in the chamber with a JUMOTM dtrans p30 pressure sensor and by monitoring the volume V of the balloon with the video of the deforming membrane. We realize the two charge reservoirs of different voltages, Φ_{in} and Φ_{out} , by using high-voltage capacitors (FTCapTM Germany) with capacitance of $C_{in} = C_{out} = 440$ nF, much larger than the maximum capacitance of the membrane $C_{max} = 34.7$ nF in the fully inflated state. The voltage of the membrane, Φ_m , is measured without electrical contact by a Kelvin probe voltmeter (TREKTM model 341 A) to avoid charge leakage through the measurement instrument. The measured voltage Φ_m is taken to be the same as the voltage of the input reservoir when it is connected to the membrane, and the slight decrease in the voltage $\Delta\Phi_{in}$ of the input reservoir determines the amount of charge drawn from the input reservoir, $\Delta Q = C_{in}\Delta\Phi_{in}$. A similar procedure determines the charge released to the output reservoir. Data acquisition is performed with a DAQ-card (National InstrumentsTM PCI-6040 E). The charge reservoirs are connected to the top electrode of the membrane via high-voltage reed relays (MederTM H12-1A69). The inlet and outlet valves as well as the relays are controlled via an USB-relay card (QUANCOMTM USBREL8/A) and a LabViewTM program.

The energy flows are shown in Fig. 1(b). The reservoir of low voltage Φ_{in} supplies electric charge to the membrane, the mechanical energy elevates the voltage of the charge, and the charge is then released to the reservoir of high voltage Φ_{out} . That is, the mechanical energy pumps electric charge from a low voltage to a high voltage.

Figure 2 shows the chosen cycle of energy conversion in a plane, whose axes are work-conjugate variables: the voltage Φ_m and the charge Q_m of the membrane. At state 1 the membrane is connected to the input reservoir at voltage Φ_{in} .

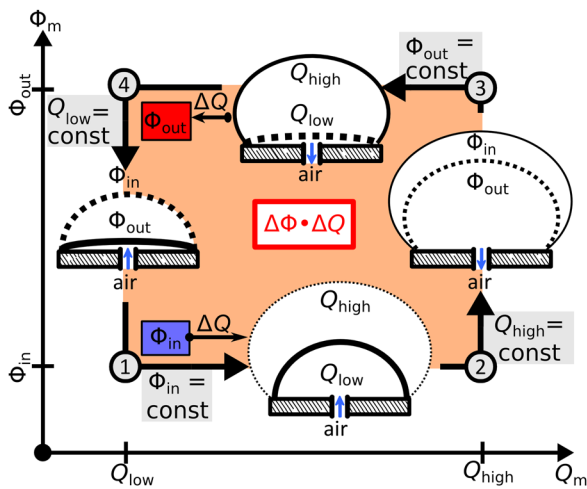


FIG. 2. (Color online) Rectangular energy conversion cycle operating between two charge reservoirs depicted in the work-conjugate (Φ, Q) plane. The cycle proceeds counterclockwise from state 1 to state 4. During the four steps of the cycle solid and dashed lines indicate the evolution of the balloon shape. In the constant voltage steps, $1 \rightarrow 2$ and $3 \rightarrow 4$, charges are taken from the low voltage reservoir and fed into the high voltage reservoir. In the constant charge steps $2 \rightarrow 3$ and $4 \rightarrow 1$, the voltage across the membrane is brought in line with the reservoirs. The area enclosed by the contour corresponds to the generated electrical energy $\Delta\Phi\Delta Q$.

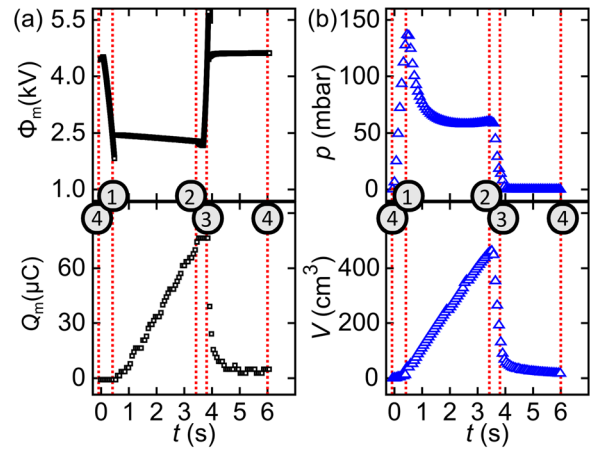


FIG. 3. (Color online) Time evolution of work-conjugate variables during one full conversion cycle. (a) Voltage Φ_m (top) and charge Q_m (bottom) on the membrane. (b) Excess pressure p (top) and volume V (bottom) of the balloon. Dashed red lines with number labels correspond to the respective states in Fig. 2.

In the isovoltic process from state 1 to state 2, the membrane at voltage Φ_{in} is inflated (the balloon shape is indicated with solid (state 1) and dashed (state 2) lines), drawing an amount of charge $\Delta Q = Q_{high} - Q_{low}$ and electrical energy $|\Delta E_{12}| = \Phi_{in}\Delta Q$ from the input reservoir. Next, the membrane is disconnected from the reservoir to work under open circuit conditions. The membrane is deflated, and hence the voltage of the membrane increases by $\Delta\Phi = \Phi_{out} - \Phi_{in}$ reaching Φ_{out} at state 3. From state 3 to state 4 the membrane is connected to the output reservoir at high voltage Φ_{out} . By releasing air in this second isovoltic step, an amount of charge ΔQ from the compliant electrodes and electrical energy $|\Delta E_{34}| = \Phi_{out}\Delta Q$ is transferred to the output reservoir. In the constant charge step under open circuit conditions from state 4 to state 1, the membrane is inflated until the electrical voltage decreases to Φ_{in} , completing the cycle. For the rectangular cycle chosen, the electrical energy generated per cycle is $E_{gen} = |\Delta E_{34}| - |\Delta E_{12}| = \Delta\Phi\Delta Q$. If the output voltage Φ_{out} and maximal volume are chosen close to the material limits (dielectric breakdown and rupture), the cycle can be used to compare the aptitude of different materials for use in DEGs.

Figure 3(a) shows the evolution of electrical work-conjugate variables: voltage Φ_m and charge Q_m . At $t = 0$ s the voltage on the membrane is $\Phi_{out} = 4.5$ kV and the charge on the electrodes is Q_{low} , corresponding to state 4 in Fig. 2. By inflating the membrane we increase the capacitance C_m and reduce the voltage Φ_m reaching $\Phi_{in} = 2.5$ kV (state 1) at $t \approx 0.48$ s. At this moment the input reservoir C_{in} is connected to the membrane. The voltage shortly falls below Φ_{in} because of control latency, with negligible effect on the harvested energy, as shown later. The slight voltage decrease $\Delta\Phi_{12}$ of the input reservoir between state 1 and 2 (between $t \approx 0.48$ s and $t \approx 3.48$ s) is used to calculate the amount of charge $\Delta Q_{12} = C_{in}\Delta\Phi_{12} = 74.36$ μ C and energy $|\Delta E_{12}| = 183$ mJ extracted from the input reservoir.

Rapid deflation (used to avoid charge leakage through the elastomer membrane) under open-circuit conditions causes the voltage to shortly rise above $\Phi_{out} = 4.5$ kV at $t \approx 3.86$ s (due to control latency), then the output reservoir

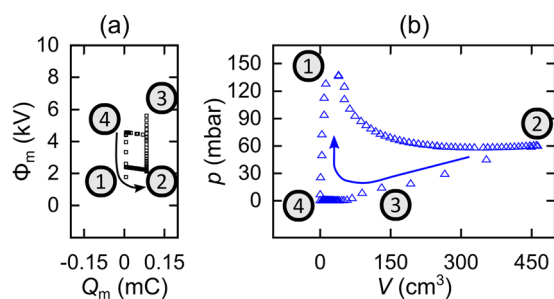


FIG. 4. (Color online) Measured cycle depicted in the (a) electrical and (b) mechanical work-conjugate plane. The areas enclosed by the contours correspond to (a) the generated electrical energy [156 mJ (102 mJ/g)] and (b) the used mechanical energy [2.08 J (1.36 J/g)].

C_{out} is connected. Applying the same approach as above, we obtain the amount of charge $\Delta Q_{34} = C_{\text{out}} \Delta \Phi_{34} = 74.32 \mu\text{C}$ and energy $|\Delta E_{34}| = 339 \text{ mJ}$ transferred to the high voltage reservoir C_{out} . Further relaxation until $t = 6 \text{ s}$ finishes the cycle, and state 4 is reached again.

The amount of charge taken from one reservoir and delivered to the other is nearly identical, revealing small leakage current losses through the membrane in the chosen cycle. This enables the calculation of the capacitance of the membrane through monitoring the voltage of the reservoirs, if charge losses are neglected.

Figure 3(b) shows the time evolution of the mechanical work-conjugate variables. During inflation of the balloon from state 4 to 2 the pressure follows the well known N-shaped equation of state for elastomer balloons.¹⁴ During deflation from state 2 to 4 the pressure drops and the balloon volume decreases close to the initial value.

The cycle of energy conversion is summarized in work-conjugate planes in Fig. 4. The scales are chosen such that identical areas in (a) and (b) correspond to equal amounts of energy. The black squares in Fig. 4(a) show the counter-clockwise path of the DEG cycle in the electrical work-conjugate (Φ, Q) plane with an enclosed area corresponding to the generated electrical energy of $E_{\text{gen}} = 156 \text{ mJ}$. The undershoots and overshoots of the voltage in state 1 and 3 cause no significant contributions to the area; thus, the control latency has negligible influence on the conversion performance.

The blue triangles in Fig. 4(b) depict the clockwise path of the DEG cycle in the (p, V) plane. The enclosed area corresponds to a mechanical work of $W_{\text{in}} = 2.08 \text{ J}$ used in the conversion process. The mechanical to electrical energy conversion efficiency of the DEG is $\eta = E_{\text{gen}}/W_{\text{in}} = 7.5\%$, equal to the ratio of the areas enclosed in the mechanical and electrical work-conjugate planes of Fig. 4. For the selected experimental parameters defining our cycle the measured specific electrical energy generated per cycle is 102 mJ/g, while the specific average power amounts to 17 mW/g.

Maximization of the specific electrical energy generated per cycle would be feasible by operating the generator close to the boundaries of the area of allowable states defined in Ref. 2. The observed mechanical to electrical energy conversion efficiency for the VHB elastomer is rather low due to significant mechanical losses, possibly caused by creep effects originating from the low cross-link density¹⁵ of the used elastomer. Prestretching the membrane may increase efficiency.

In summary we have developed an experiment to monitor energy flows in DEGs. We use large capacitors as input and output charge reservoirs to measure electrical energy flows, obtaining the specific electrical energy generated per cycle and the specific average power. The cycles presented in work-conjugate planes visualize the mechanical to electrical energy conversion efficiency. If the DEG is operated close to the material limits the experiment can be used to analyze the maximum specific electrical energy generated per cycle and mechanical to electrical conversion efficiency, allowing for a comparison of the aptitude of different materials for energy harvesting. Our method to monitor electrical energy flows with finite charge reservoirs can be readily employed for different designs of DEGs. Future work will focus on the study of the effects of prestrain, different generator designs, and loss mechanisms on the generated energy and efficiency.

This work was partially supported by the Austrian Science Fund (FWF-P22912-N20). The work at Harvard is supported by the NSF through a grant on Soft Active Materials (CMMI-0800161) and by the MURI through a contract on Adaptive Structural Materials (W911NF-09-1-0476).

¹R. Pelrine, R. D. Kornbluh, J. Eckerle, P. Jeuck, S. Oh, Q. Pei, and S. Stanford, *Proc. SPIE* **4329**, 148 (2001).

²S. J. A. Koh, X. Zhao, and Z. Suo, *Appl. Phys. Lett.* **94**, 262902 (2009).

³R. Pelrine, R. D. Kornbluh, Q. Pei, and J. Joseph, *Science* **287**, 836 (2000).

⁴F. Carpi, S. Bauer, and D. De Rossi, *Science* **330**, 1759 (2010).

⁵R. D. Kornbluh, R. Pelrine, H. Prahlad, A. Wong-Foy, B. McCoy, S. Kim, J. Eckerle, and T. Low, *Proc. SPIE* **7976**, 797605 (2011).

⁶S. J. A. Koh, C. Keplinger, T. Li, S. Bauer, and Z. Suo, *IEEE/ASME Trans. Mechatron.* **16**, 33 (2011).

⁷T. McKay, B. O'Brien, E. Calius, and I. Anderson, *Proc. SPIE* **7642**, 764216 (2010).

⁸T. McKay, B. M. O'Brien, E. Calius, and I. Anderson, *Smart Mater. Struct.* **19**, 055025 (2010).

⁹T. G. McKay, B. M. O'Brien, E. P. Calius, and I. Anderson, *Appl. Phys. Lett.* **98**, 142903 (2011).

¹⁰C. Jean-Mistral, S. Basrour, and J.-J. Chaillout, *Proc. SPIE* **6927**, 692716 (2008).

¹¹C. Graf and J. Maas, *Proc. SPIE* **7976**, 79760H (2011).

¹²J. W. Fox and N. Goulbourne, *J. Mech. Phys. Solids* **56**, 2669 (2008).

¹³A. Koh, *MRS Proc.* **1218**, 1218-Z07-10 (2009).

¹⁴I. Müller and P. Strehlow, *Rubber and Rubber Balloons: Paradigms of Thermodynamics (Lecture Notes In Physics 637)* (Springer, Heidelberg, 2004), p. 4.

¹⁵J. G. Curro and P. Pincus, *Macromolecules* **16**, 559 (1983).